

Gapless spin-liquid ground state in the $S = 1/2$ kagome antiferromagnet

H. J. Liao,¹ Z. Y. Xie,^{1,2} J. Chen,¹ Z. Y. Liu,³ H. D. Xie,¹ R. Z. Huang,¹ B. Normand,^{4,2} and T. Xiang^{1,5,*}

¹*Institute of Physics, Chinese Academy of Sciences, P.O. Box 603, Beijing 100190, China*

²*Department of Physics, Renmin University of China, Beijing 100872, China*

³*Institute of Theoretical Physics, Chinese Academy of Sciences, P.O. Box 2735, Beijing 100190, China*

⁴*Laboratory for Neutron Scattering and Imaging,*

Paul Scherrer Institute, CH-5232 Villigen PSI, Switzerland

⁵*Collaborative Innovation Center of Quantum Matter, Beijing 100190, China*

(Dated: March 1, 2017)

The defining problem in frustrated quantum magnetism, the ground state of the nearest-neighbor $S = 1/2$ antiferromagnetic Heisenberg model on the kagome lattice, has defied all theoretical and numerical methods employed to date. We apply the formalism of tensor-network states (TNS), specifically the method of projected entangled simplex states (PESS), which combines infinite system size with a correct accounting for multipartite entanglement. By studying the ground-state energy, the finite magnetic order appearing at finite tensor bond dimensions, and the effects of a second-neighbor coupling, we demonstrate that the ground state is a gapless spin liquid. We discuss the comparison with other numerical studies and the physical interpretation of this result.

In one spatial dimension (1D), quantum fluctuations dominate any physical system and semiclassical order is destroyed. In higher dimensions, frustrated quantum magnets offer perhaps the cleanest systems for seeking the same physics, including quantum spin-liquid states, fractionalized spin degrees of freedom, and exotic topological properties. This challenge has now become a central focus of efforts spanning theory, numerics, experiment, and materials synthesis [1–4]. While much has been understood about frustrated systems on the triangular, pyrochlore, Shastry-Sutherland, and other 2D and 3D lattices, it is fair to say that the ground-state properties of the $S = 1/2$ kagome Heisenberg antiferromagnet (KHAF) remain a complete enigma.

An analytical Schwinger-boson approach [5], coupled-cluster methods [6], and density-matrix renormalization-group (DMRG) calculations [7–9], including analysis of the topological entanglement entropy [10], all suggest a gapped spin liquid of Z_2 topology. The most sophisticated DMRG studies [9, 11] estimate a triplet spin gap $\Delta \geq 0.05J$. Analytical large- N expansions [12] and numerical simulations by variational Monte Carlo (VMC) [13, 14] suggest a gapless spin liquid with $U(1)$ symmetry and a Dirac spectrum of spinons. Extensive exact-diagonalization calculations conclude that the accessible system sizes are simply too small to judge [15, 16]. Debate continues between the gapped Z_2 and gapless $U(1)$ scenarios, with very recent arguments in support of both [17, 18], while a symmetry-preserving TNS study favors the gapped Z_2 ground state [19]. Experimental approaches to the kagome conundrum have made considerable progress in recent years, but for the purposes of the current theoretical analysis we defer a review to Sec. SI of the Supplementary Material (SM) [20].

In this Letter, we employ the PESS description of the entangled many-body ground state to compute the properties of the KHAF. Because we consider an infinite sys-

tem, our results provide hitherto unavailable insight. As functions of the finite tensor bond dimension, we find algebraic convergence of the ground-state energy and algebraic vanishing of a finite staggered magnetization, indicating a gapless spin liquid. We demonstrate that the phase diagram in the presence of next-neighbor coupling contains a finite region of this spin-liquid phase. Our results suggest that the physics of the KHAF is driven by maximizing the kinetic energy of gapless Dirac spinons.

The TNS formalism is based on expressing the wave function as a generalized matrix-product state (MPS) [52–54]. As we review in Sec. SII of the SM [20], this Ansatz obeys the area law of entanglement and, crucially, allows the construction of a renormalization-group scheme to reach the limit of infinite lattice size. The truncation parameter is the tensor bond dimension, D . We introduced the PESS formulation [55] in order to capture the multipartite entanglement within each lattice unit, or simplex [55–57], which is the key element of frustrated systems and is missing in the conventional pairwise projected entangled pair states (PEPS) construction. Summarizing the numerical procedure (Sec. SII [20]), the optimized PESS approach is a projection technique, with tensor manipulation performed by higher-order singular-value decomposition (HOSVD), and freedom to choose the simplex, the unit cell, and a simple- or full-update treatment of the bond environment during tensor renormalization, the former allowing access to larger D but the latter achieving more rapid convergence.

However, TNS calculations are a two-step process, where the wave function is obtained first and then used to calculate physical expectation values. This latter step requires projection onto a 1D MPS basis, whose dimension for convergence is found to scale approximately as $D_{\text{mps}} \approx 4D^2$. Once $D \gtrsim 15$, the evaluation step becomes the more computationally intensive problem, and here we implement new methodology (outlined in Sec. SII [20]) by

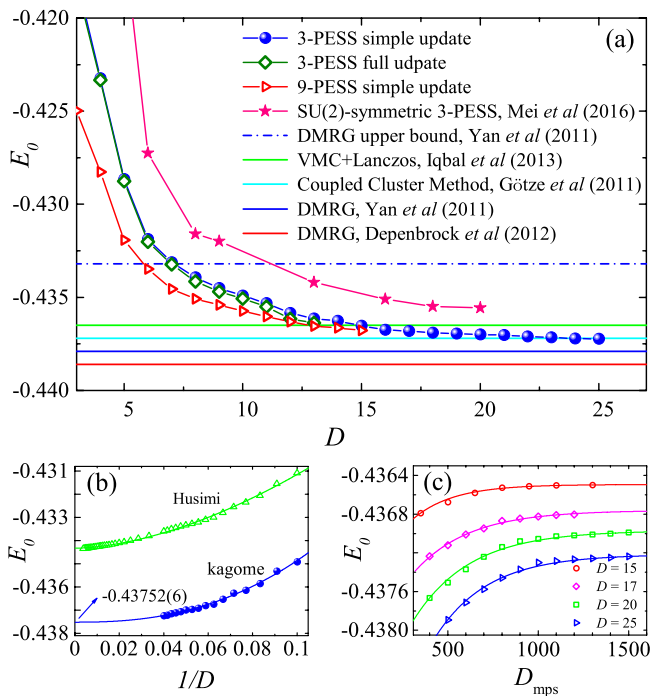


FIG. 1. **Ground-state energy of the KHAF.** (a) E_0 as a function of D , shown for the 3-PESS and simple-update method up to $D = 25$, 3-PESS by full update to $D = 13$, and 9-PESS with simple update to $D = 15$. Shown for comparison are results from other numerical studies. (b) $E_0(D)$ for the 3-PESS, shown as a function of $1/D$ and compared with results obtained for the Husimi lattice [57]. (c) Convergence of $E_0(D)$ as a function of D_{mps} , shown for several values of D .

which we extend the accessible D range.

We begin by presenting results from the 3-site-simplex (3-PESS) Ansatz for all accessible D values. The ground-state energy, $E_0(D)$, of the nearest-neighbor KHAF is shown in Fig. 1(a). At large D , our estimate lies below those obtained from all known techniques other than DMRG studies of specific clusters, which are not an upper bound. We remark that our $E_0(D)$ values are significantly lower than those of an SU(2)-invariant TNS analysis [19]. We find that $E_0(D)$ converges algebraically with D , as on the Husimi lattice [57], indicating a gapless ground state [58]. The power-law form $E_0(D) = e_0 + aD^{-\alpha}$, shown in Fig. 1(b), delivers our best estimate of the ground-state energy, $e_0 = -0.43752(6)J$. Figure 1(c) illustrates the convergence of $E_0(D_{\text{mps}})$ for selected values of D ; we note that this part of the process is not variational and comment in detail in Sec. SII of the SM [20]. Optimized fits to a regime of exponential convergence in D_{mps} were used to extrapolate towards the values of $E_0(D)$ shown in Figs. 1(a) and 1(b), and to determine the associated error bars, on the basis of which we limit our claims of reliability to $D \leq 25$.

One key qualitative property of our PESS wave func-

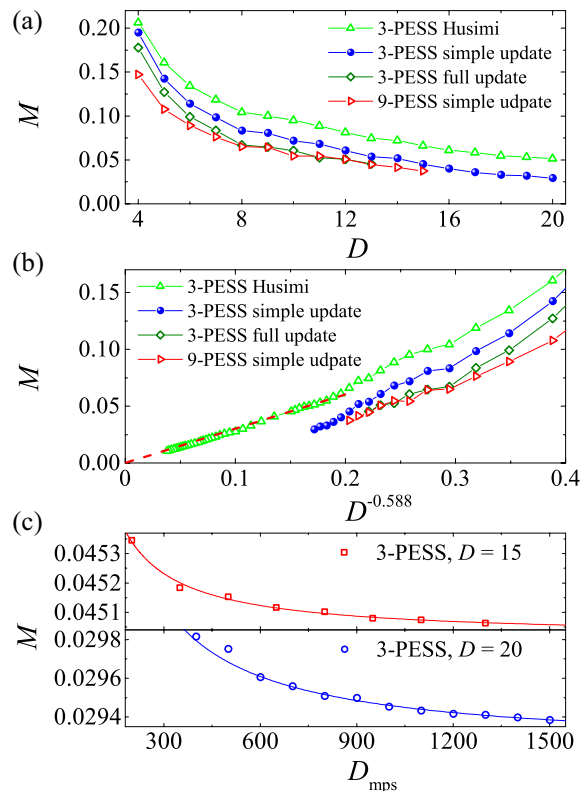


FIG. 2. **Staggered magnetization of the KHAF at finite D .** (a) M as a function of D , shown for the 3-PESS and simple-update method up to $D = 20$, 3-PESS by full update to $D = 13$, and 9-PESS with simple update to $D = 15$. Shown for comparison are results obtained for the Husimi lattice [57]. (b) M as a function of $1/D^{0.588}$, the power-law form obtained for the Husimi lattice. (c) Convergence of $M(D)$ as a function of D_{mps} , shown for $D = 15$ and $D = 20$.

tion is a finite 120° magnetic order at all finite D values, as shown in Figs. 2(a) and 2(b). The order parameter, $M(D)$, varies algebraically with $1/D$ over the available D range, tending to zero as $D \rightarrow \infty$, as required of a spin liquid. Figure 2(c) illustrates the convergence of $M(D_{\text{mps}})$ for $D = 15$ and 20 , where an algebraic form was deduced from the truncation error, and reliable extrapolations to large D_{mps} were obtained only for $D \leq 20$.

The Husimi lattice provides essential confirmation of our results. It possesses the same local physics as the kagome lattice, but less frustration from longer paths, and it allows PESS calculations up to $D = 260$, yielding accurate extrapolations to the large- D limit [57]. It confirms the crucial qualitative statement that magnetically ordered states have the lowest energies for spatially infinite systems at finite D . It benchmarks the algebraic nature of $E_0(D)$ [Fig. 1(b)] and $M(D)$ [Fig. 2(b)], the latter vanishing exactly at large D . The Husimi $M(D)$ sets an upper bound on the kagome $M(D)$ (Sec. SIII of the SM [20]). Our kagome results lie well below this bound,

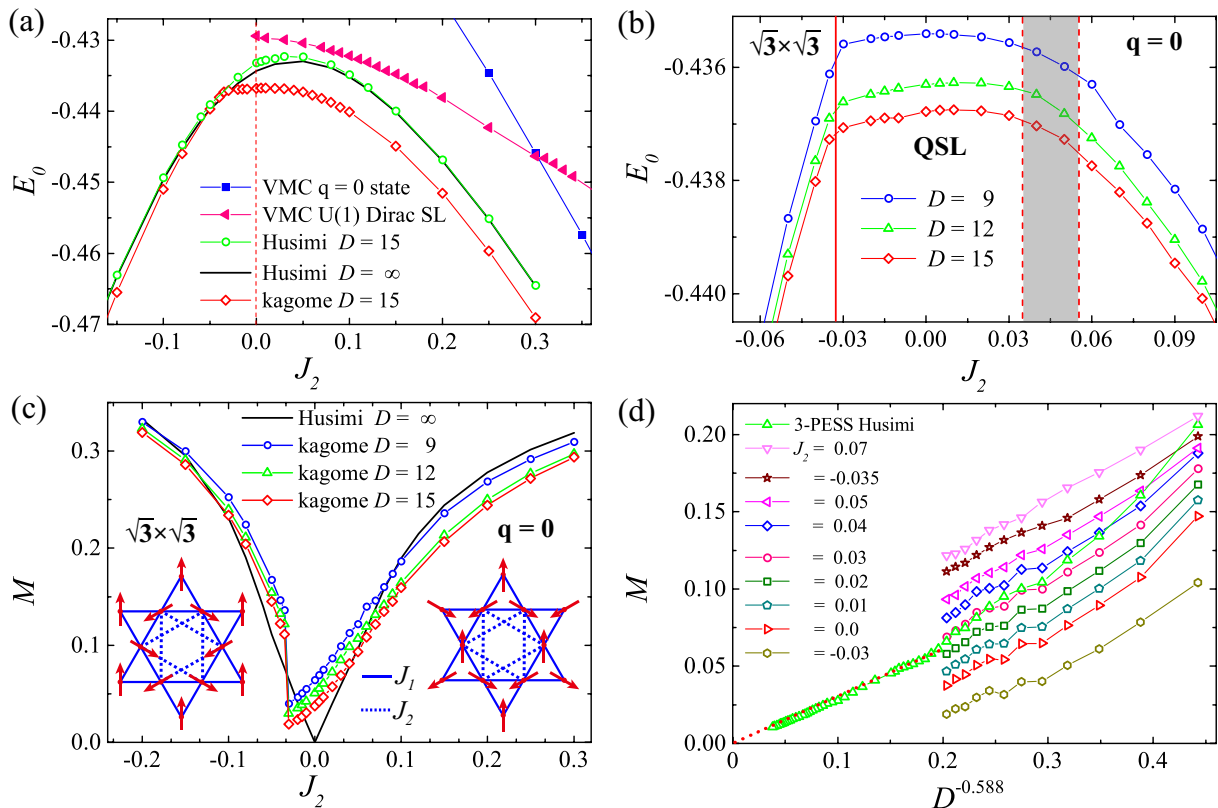


FIG. 3. **Energy and staggered magnetization of the KHAF with next-neighbor coupling.** (a) $E_0(J_2)$ calculated with a 9-PSS using $D = 15$. Shown for comparison are results for the Husimi lattice with $D = 15$ and $D = \infty$, as well as the VMC results of Ref. [14]. (b) Detail of $E_0(J_2)$ near $J_2 = 0$; with increasing D , a cusp-type discontinuity emerges near $J_2 = -0.03$ (red solid line). The shaded region denotes the location of the continuous transition at small positive J_2 , deduced from the magnetization of panel (d). (c) $M(J_2)$ calculated using $D = 9, 12$, and 15 , compared with results for the Husimi lattice at $D = \infty$. Insets represent the $\sqrt{3} \times \sqrt{3}$ (left) and $q = 0$ ordered phases (right). (d) M as a function of $1/D^{0.588}$, with the Husimi result indicating J_2 values for which M may extrapolate to zero within the error bars.

but with no evidence for deviation from a similar algebraic form, reinforcing the conclusion that the ground state of the KHAF is a gapless spin liquid.

For full rigor we consider every aspect of the PSS procedure. Full-update calculations confirm the accuracy of the simple-update approximation for all accessible D values. $E_0(D)$ lies only slightly lower [Fig. 1(a)], with no change in functional form; similarly, $M(D)$ is suppressed by several percent [Figs. 2(a) and 2(b)], reinforcing the argument for convergence to $M = 0$ at large D , but still shows algebraic behavior. To investigate whether magnetic order might be artificially enhanced by the 3-PSS, in Figs. 1(a), 2(a), and 2(b) we also present results obtained using a 9-site simplex (9-PSS) [55], which again confirm the algebraic form of $E_0(D)$ and $M(D)$, with no evidence either of a crossover to exponential behavior of $E_0(D)$ or of a collapse of $M(D)$ to zero at finite D . 3-PSS calculations may be performed with a unit cell containing any number of simplices (Sec. SII [20]); our results for 3-, 9-, and 12-site unit cells are identical, again confirming no inherent bias of this type.

Further essential confirmation is obtained by adding a next-neighbor coupling, J_2 . These calculations are performed most efficiently with a 9-PSS and we reach $D = 15$ with simple updates. As shown in Fig. 3(a), $E_0(J_2)$ is maximal (the system is most frustrated) close to $J_2 = 0$ and is not symmetrical about this point. For the Husimi lattice, $E_0(J_2)$ is continuous, with maximal frustration at $J_2 \simeq 0.04$. By contrast, the kagome case shows a regime of almost constant energy when $-0.03 \lesssim J_2 \lesssim 0.04$ [Fig. 3(b)]. To understand the nature of these states, we consider in Fig. 3(c) the finite- D magnetization and in Fig. 3(d) $M(D)$ for selected values of J_2 . For the Husimi lattice, $M(J_2)$ is zero only at $J_2 = 0$, where it has a discontinuity, and [despite the form of $E_0(J_2)$] is almost symmetrical. For kagome, the expected ordered phases are the $q = 0$ structure at $J_2 > 0$ and the $\sqrt{3} \times \sqrt{3}$ structure at $J_2 < 0$ [Fig. 3(c)]. However, $M(J_2)$ at finite D continues to fall through $J_2 = 0$ from above, indicating a region of $q = 0$ order at $J_2 < 0$, which is terminated at $J_2 \simeq -0.03$ by a discontinuous jump to $\sqrt{3} \times \sqrt{3}$ order. From Fig. 3(d), $M(D)$ appears

to extrapolate to zero over a range of J_2 values, which we estimate from the Husimi magnetization to be fully consistent with the “plateau” in $E(J_2)$ [Fig. 3(b)].

The gapless spin liquid should exist over a finite range of J_2 if it is a robust quantum ground state. The Husimi case, with magnetic order at all finite values of $|J_2|$ and a spin liquid only at the single point $J_2 = 0$, is a type of “phase diagram” allowed only because of the pathological Husimi geometry. In the kagome case, indeed we find a finite disordered regime, bounded by a first-order transition at $J_2 \simeq -0.03$ and an apparent second-order transition at $J_2 = 0.045 \pm 0.01$. Evidently the additional quantum fluctuations due to the presence of loops in the kagome geometry act to create the same gapless spin-liquid ground state as the nearest-neighbor model ($J_2 = 0$, Figs. 1 and 2). Our results are in qualitative accord with those proposed in Ref. [14] on the basis of VMC studies of a finite system, although quantitatively the range of stability we deduce is much narrower.

PESS can be used to calculate further ground-state expectation values. However, the finite $M(D)$ means that the field-induced magnetization contains no information useful at zero field. Similarly, finite- D correlation functions have a constant part, which masks the nontrivial power-law behavior expected of a gapless spin liquid. We have nevertheless obtained definitive numerical results, in the thermodynamic limit, for the two key characteristic quantities, $E_0(D, J_2)$ and $M(D, J_2)$. Although our method is based on gapped states, it is able to indicate its own “breakdown” in the event of continuing algebraic convergence [58], and thus the conclusion of a gapless spin-liquid ground state is robust.

To interpret the physical implications of this result, the leading candidate gapless wave function is the U(1) Dirac-fermion state proposed in Ref. [12]. Although there exist gapless Z_2 spin-liquid states of the KHAF [59], there is currently neither numerical evidence [14] nor a physical argument in support of these. Heuristically, gapped spin liquids are favored by the formation of low-energy local states, such as dimer or plaquette singlets, whereas systems with a net odd-half-integer spin per simplex do not offer this option. Our results imply that there is no local unit (such as the hexagon) on the kagome lattice, and instead the optimal energy is gained by maximizing the kinetic energy of mobile spinons, leading to the U(1) Dirac-fermion state [12], or by maximizing the contributions from gauge fluctuations [60]. The gapless spin liquid is expected to have long-ranged entanglement and correlation functions [61], and the U(1) state has no well-characterized topological order.

Turning to the general question of numerical KHAF studies, our results constitute a major breakthrough because of the infinite system size. The fact that all ED and DMRG studies consistently favor gapped states suggests that systems finite even in only one dimension are not able to account appropriately for spinon kinetic-energy

contributions. Regarding the question of enforced or emerging spin symmetries, PESS studies enforcing U(1) [62] or SU(2) [19] symmetry find gapped states with energies higher than ours (Fig. 1). In our calculations, it is straightforward to start with a gapped trial PESS wave function and show that an ordered state of lower energy emerges on projection. In fact all starting wave functions (symmetric, ordered, arbitrary) lead to the same final state for a given simplex and update type, with $E_0(D)$ and $M(D)$ as shown in Figs. 1 and 2. Thus it appears that symmetry-enforcing studies are finding excited states, and it is likely that the same applies on finite systems. Indeed it is argued in Ref. [18] that a gapped Z_2 ground state can lie at lower energy than the gapless U(1) state on a finite system, but not in the thermodynamic limit. A very recent study using VMC evaluation of TNS wave functions on finite systems also supports a U(1) rather than any competing Z_2 state [63].

Clearly the KHAF is a problem where competing states of very different character lie very close in energy. We deduce that the large- N approach offers the best available account of quantum fluctuation effects, specifically by capturing the kinetic-energy gain of mobile spinons. Our results also demonstrate the qualitative value of the VMC calculations [14], which arrive at the gapless spin-liquid ground state by a different route from PESS, without allowing states of finite M . It is also essential to benchmark whether the PESS Ansatz is “neutral” in its energy accounting, and does not over-emphasize gapless or ordered states, a question we addressed by comparing the 3- and 9-PESS results in Figs. 1(a) and 2(a).

A further question is whether the algebraic convergence we observe could cross over to exponential beyond the range of our PESS calculations. If such a crossover were to begin at $D = 26$, it is hard to argue [consider Fig. 1(b)] that the difference in extrapolated ground-state energies could exceed $\Delta E = 0.0001J$. One is then faced with the emergence of an extremely small energy scale for no apparent reason. This minuscule energy would have to be the spin gap of the corresponding Z_2 state, but clearly lies far below the DMRG gap. ΔE lies well below the “stabilization energy” of any of the competing states, whether they arise due to local resonances, spinon kinetic energy, gauge fluctuations, or any other mechanism.

Turning briefly to experiment, some studies of the material herbertsmithite, which offers Cu^{2+} ions in an ideal kagome geometry, have indeed suggested a continuum of fractional spin excitations (Sec. SI of the SM [20]). However, the most recent measurements face competing gapped [64, 65] and gapless [66, 67] interpretations. In addition, it remains unclear whether, due to interplane disorder and Dzyaloshinskii-Moriya interactions, this material is providing a true reflection of kagome physics.

In summary, we have used the method of projected entangled simplex states to demonstrate that the ground state of the Heisenberg antiferromagnet for $S = 1/2$

spins on the kagome lattice with only nearest-neighbor interactions is a gapless quantum spin liquid. A finite next-neighbor interaction reveals the presence of a narrow regime of gapless spin liquid between states of finite 120° staggered magnetic order. This spin liquid is thought to be the U(1) Dirac-fermion state, in which the primary driving force for spin-liquid behavior is the maximization of spinon kinetic energy.

We thank L. Balents, F. Becca, M. Hermele, and W. Li for helpful discussions. This work was supported by the National Natural Science Foundation of China (Grant Nos. 10934008, 10874215, and 11174365), by the National Basic Research Program of China (Grant Nos. 2012CB921704 and 2011CB309703), and by the Ministry of Science and Technology of China (Grant No. 2016YFA0300503).

* txiang@iphy.ac.cn

- [1] L. Balents, *Nature* **464**, 199-208 (2010).
- [2] P. Mendels and A. S. Wills, in *Introduction to Frustrated Magnetism*, eds. C. Lacroix, P. Mendels, and F. Mila (Springer, Heidelberg, 2011).
- [3] K. Kanoda and R. Kato, *Annu. Rev. Condens. Matter Phys.* **2**, 167 (2011).
- [4] B. Normand, *Contemp. Phys.* **50**, 4, 533 (2009).
- [5] S. Sachdev, *Phys. Rev. B* **45**, 12377 (1992).
- [6] O. Götze, D. J. J. Farnell, R. F. Bishop, P. H. Y. Li, and J. Richter, *Phys. Rev. B* **84**, 224428 (2011).
- [7] H. C. Jiang, Z. Y. Weng, and D. N. Sheng, *Phys. Rev. Lett.* **101**, 117203 (2008).
- [8] S. Yan, D. A. Huse, and S. R. White, *Science* **332**, 1173 (2011).
- [9] S. Depenbrock, I. P. McCulloch, and U. Schollwöck, *Phys. Rev. Lett.* **109**, 067201 (2012).
- [10] H. C. Jiang, Z. H. Wang, and L. Balents, *Nat. Phys.* **8**, 902 (2012).
- [11] S. Nishimoto, N. Shibata, and C. Hotta *Nat. Commun.* **4**, 2287 (2013).
- [12] Y. Ran, M. Hermele, P. A. Lee, and X. G. Wen, *Phys. Rev. Lett.* **98**, 117205 (2007).
- [13] Y. Iqbal, F. Becca, S. Sorella, and D. Poilblanc, *Phys. Rev. B* **87**, 060405 (2013).
- [14] Y. Iqbal, D. Poilblanc, and F. Becca, *Phys. Rev. B* **91**, 020402(R) (2015).
- [15] P. Sindzingre and C. Lhuillier, *Eur. Phys. Lett.* **88**, 27009 (2009).
- [16] A. M. Läuchli, J. Sudan, and R. Moessner, unpublished (arXiv:1611.06990).
- [17] T. Li, unpublished (arXiv:1601.02165).
- [18] Y. Iqbal, D. Poilblanc, and F. Becca, unpublished (arXiv:1606.02255).
- [19] J.-W. Mei, J.-Y. Chen, H. He, and X.-G. Wen, unpublished (arXiv:1606.09639).
- [20] For details see the Supplemental Material, which includes Refs. [21] to [51]
- [21] M. P. Shores, E. A. Nytko, B. M. Bartlett, and D. G. Nocera, *J. Am. Chem. Soc.* **127**, 13462 (2005).
- [22] M. Rigol and R. R. P. Singh, *Phys. Rev. Lett.* **98**, 207204 (2007).
- [23] G. Misguich and P. Sindzingre, *Eur. Phys. J. B* **59**, 305 (2007).
- [24] P. Mendels, F. Bert, M. A. de Vries, A. Olariu, A. Harrison, F. Duc, J.-C. Trombe, J. S. Lord, A. Amato, and C. Baines, *Phys. Rev. Lett.* **98**, 077204 (2007).
- [25] J. S. Helton, K. Matan, M. P. Shores, E. A. Nytko, B. M. Bartlett, Y. Yoshida, Y. Takano, A. Suslov, Y. Qiu, J.-H. Chung, D. G. Nocera, and Y. S. Lee, *Phys. Rev. Lett.* **98**, 107204 (2007).
- [26] A. Olariu, P. Mendels, F. Bert, F. Duc, J. C. Trombe, M. A. de Vries, and A. Harrison, *Phys. Rev. Lett.* **100**, 087202 (2008).
- [27] T. H. Han, J. S. Helton, S. Chu, A. Prodi, D. K. Singh, C. Mazzoli, P. Müller, D. G. Nocera, and Y. S. Lee, *Phys. Rev. B* **83**, 100402(R) (2011).
- [28] A. Zorko, S. Nellutla, J. van Tol, L. C. Brunel, F. Bert, F. Duc, J. C. Trombe, M. A. de Vries, A. Harrison, and P. Mendels, *Phys. Rev. Lett.* **101**, 026405 (2008).
- [29] O. Cépas, C. M. Fong, P. W. Leung, and C. Lhuillier, *Phys. Rev. B* **78**, 140405 (R) (2008).
- [30] I. Rousochatzakis, S. Manmana, A. Läuchli, B. Normand, and F. Mila, *Phys. Rev. B* **79**, 214415 (2009).
- [31] S. Dommange, M. Mambrini, B. Normand, and F. Mila, *Phys. Rev. B* **68**, 224416 (2003).
- [32] A. Läuchli, S. Dommange, B. Normand, and F. Mila, *Phys. Rev. B* **76**, 144113 (2007).
- [33] S.-H. Lee, H. Kikuchi, Y. Qiu, B. Lake, Q. Huang, K. Habicht, and K. Kiefer, *Nat. Mater.* **6**, 853 (2007).
- [34] M. A. de Vries, K. V. Kamenev, W. A. Kockelmann, J. Sanchez-Benitez, and A. Harrison, *Phys. Rev. Lett.* **100**, 157205 (2008).
- [35] F. Bert, S. Nakamae, F. Ladieu, D. L'Hôte, P. Bonville, F. Duc, J.-C. Trombe, and P. Mendels, *Phys. Rev. B* **76**, 132411 (2007).
- [36] D. E. Freedman, T. H. Han, A. Prodi, P. Müller, Q.-Z. Huang, Y.-S. Chen, S. M. Webb, Y. S. Lee, T. M. McQueen, and D. G. Nocera, *J. Am. Chem. Soc.* **132**, 16185 (2010).
- [37] Z. Hiroi, M. Hanawa, N. Kobayashi, M. Nohara, H. Takagi, Y. Kato, and M. Takigawa, *J. Phys. Soc. Jpn.* **70**, 3377 (2001).
- [38] H. Ishikawa, Y. Okamoto, and Z. Hiroi, *J. Phys. Soc. Jpn.* **82**, 063710 (2013).
- [39] E. A. Nytko, J. S. Helton, P. Müller, and D. G. Nocera, *J. Am. Chem. Soc.* **130**, 2922 (2008).
- [40] Y. Okamoto, H. Yoshida, and Z. Hiroi, *J. Phys. Soc. Jpn.* **78**, 033701 (2009).
- [41] H. R. Oswald, *Helv. Chim. Acta.* **52**, 2369 (1969).
- [42] J. Eisert, M. Cramer, and M. B. Plenio, *Rev. Mod. Phys.* **82**, 277 (2010).
- [43] F. Pollmann, S. Mukerjee, A. Turner, and J. E. Moore, *Phys. Rev. Lett.* **102**, 255701 (2009).
- [44] M. P. Nightingale and J. C. Umrigar, *Quantum Monte Carlo Methods in Physics and Chemistry*, Springer (1999).
- [45] G. Vidal, *Phys. Rev. Lett.* **91**, 147902 (2003); G. Vidal, *Phys. Rev. Lett.* **93**, 040502 (2004).
- [46] M. Lubasch, J. I. Cirac, and M.-C. Banuls, *Phys. Rev. B* **90**, 064425 (2014); H. N. Phien, J. A. Benghwa, H. D. Tuan, P. Corboz, and R. Orus, *Phys. Rev. B* **92**, 035142 (2015).
- [47] H. C. Jiang, Z. Y. Weng, and T. Xiang, *Phys. Rev. Lett.* **101**, 090603 (2008).

- [48] W. Li, J. Von Delft, and T. Xiang, Phys. Rev. B **86**, 195137 (2012).
- [49] H. H. Zhao, Z. Y. Xie, Q. N. Chen, Z. C. Wei, J. W. Cai, and T. Xiang, Phys. Rev. B **81**, 174411 (2010); R. Orus, Ann. Phys. **349**, 117 (2014).
- [50] G. Vidal, Phys. Rev. Lett. **98**, 070201 (2007); R. Orus, and G. Vidal, Phys. Rev. B **78**, 155117 (2008); J. Jordan, R. Orus, G. Vidal, F. Verstraete, and J. I. Cirac, Phys. Rev. Lett. **101**, 250602 (2008).
- [51] Z. Y. Xie, H. J. Liao, Z. Y. Liu, R. Z. Huang, H. D. Xie, J. Chen, and T. Xiang, unpublished.
- [52] H. Niggemann, A. Klümper, and J. Zittartz, Z. Phys. B **104**, 103 (1997);
- [53] T. Nishino, Y. Hieida, K. Okunishi, N. Maeshima, Y. Akutsu, and A. Gendiar, Prog. Theor. Phys. **105**, 409 (2001).
- [54] F. Verstraete and J. I. Cirac, unpublished (arXiv:cond-mat/0407066).
- [55] Z.-Y. Xie, J. Chen, J.-F. Yu, X. Kong, B. Normand, and T. Xiang, Phys. Rev. X **4**, 011025 (2014).
- [56] D. P. Arovas, Phys. Rev. B **77**, 104404 (2008).
- [57] H. J. Liao, Z. Y. Xie, J. Chen, X. J. Han, H. D. Xie, B. Normand, and T. Xiang, Phys. Rev. B **93**, 075154 (2016).
- [58] B. Pirvu, G. Vidal, F. Verstraete, and L. Tagliacozzo, Phys. Rev. B **86**, 075117 (2012).
- [59] Y.-M. Lu, Y. Ran, and P. A. Lee, Phys. Rev. B **83**, 224413 (2011).
- [60] Y.-C. He, Y. Fuji, and S. Bhattacharjee, unpublished (arXiv:1512.05381).
- [61] M. Hermele, Y. Ran, P. A. Lee, and X. G. Wen, Phys. Rev. B **77**, 224413 (2008).
- [62] W. Li, private communication.
- [63] S. Jiang, P. Kim, J. H. Han, and Y. Ran, unpublished (arXiv:1610.02024).
- [64] M.-X. Fu, T. Imai, T.-H. Han, and Y. S. Lee, Science **350**, 655 (2015).
- [65] T.-H. Han, M. R. Norman, J.-J. Wen, J. A. Rodriguez-Rivera, J. S. Helton, C. Broholm, and Y. S. Lee, Phys. Rev. B **94**, 060409 (2016).
- [66] T.-H. Han, J. S. Helton, S.-Y. Chu, D. G. Nocera, J. A. Rodriguez-Rivera, C. Broholm, and Y. S. Lee, Nature **492**, 406 (2012).
- [67] P. Khuntia *et al.*, unpublished.

SUPPLEMENTAL MATERIAL

Gapless spin-liquid ground state in the $S = 1/2$ kagome antiferromagnet

H. J. Liao, Z. Y. Xie, J. Chen, Z. Y. Liu, H. D. Xie, R. Z. Huang, B. Normand, and T. Xiang

SI. Kagome Materials and Experiment

From the standpoint of materials synthesis, great strides have been made towards a pure $S = 1/2$ kagome system. $\text{ZnCu}_3(\text{OH})_6\text{Cl}_2$ (herbertsmithite) [21] offers a structurally perfect realization composed of Cu^{2+} ions. Despite the large antiferromagnetic exchange, $J \simeq 170$ -190 K [22, 23], in experiment there is no evidence of long-ranged magnetic order or even of spin freezing at any temperature down to 50 mK [24, 25]. There is also no sign of a spin gap in the excitation spectrum of powder samples [25, 26]. Even with the availability of single crystals [27], the situation remains unresolved: neutron spectroscopy [66] shows a continuum of fractional excitations and the system was suggested to be gapless (although the upper limit was set only at $\Delta/J \leq 0.1$), but was more recently interpreted as a gapped state with correlated impurities [65]. Similarly, nuclear magnetic resonance studies have been interpreted as showing a small gap ($\Delta/J \approx 0.05$) [64], but also as providing no solid evidence for the presence of one [67]. However, the physics of herbertsmithite may in fact be controlled by Dzyaloshinskii-Moriya (DM) interactions [28–30] and, although in-plane defects [30–35] have been excluded [36], there remain possible in-plane polarization and inter-plane coupling effects due to out-of-plane defects. Elsewhere, candidate $S = 1/2$ kagome materials include volborthite [37] and edwardsite [38], which have distorted lattices, $\text{Cu}(1,3\text{bdc})$ [39], which is ferromagnetic, and vesignieite [40] and Cd -kapellasite [41], which are known to have strong DM interactions, but all raise the pressure for a theoretical solution to the kagome problem before a definitive experimental one emerges.

SII. TNS-PESS Calculations

TNS and PESS

The ability to express a physical system as a tensor network has led to significant progress in fields as diverse as quantum gravity and quantum information. The power of tensor manipulation techniques (contraction, decomposition, and generalized diagonalization) offers new calculational capabilities for states and operators, as well as new insight into their physical content. In condensed matter systems, the quantity expressed as a tensor net-

work is the partition function of a classical system or the wave function of a quantum system. The TNS construction [52–54] is amenable to a renormalization-group approach which allows direct access to the thermodynamic limit of infinite lattice size, giving TNS methods a fundamental qualitative advantage over all other numerical approaches to date.

The TNS wave function respects by construction the area law of entanglement entropy [42], i.e. its entanglement content is local, which provides an Ansatz that can be computed in polynomial instead of exponential time. The truncation parameter is the tensor bond dimension, D , which is the number of auxiliary virtual degrees of freedom [54, 55] introduced on each lattice bond to describe the local physical degrees of freedom. Heuristically, D is related to the range of entanglement contained in the wave function [43], with larger D ensuring a more accurate representation. The conventional formulation of the entangled TNS wave function, PEPS, places virtual maximally entangled pairs of auxiliary particles on every bond. However, this pairwise construction does not contain the multipartite entanglement that is the hallmark of strongly frustrated systems, whence the requirement for the PESS Ansatz [55] to allow the full and efficient application of TNS to this class of problem. We comment in this context that TNS methods are free of any sign problem [44].

Updates, Simplices, and Unit Cells

The PESS representation is determined by imaginary-time evolution [45] with an arbitrary starting wave function. In updating the PESS wave function after each projection step (implemented as a small time step), one may attempt to include the full system, or bond environment, in a self-consistent manner by the full-update (FU) scheme [46], or neglect it within the simple-update (SU) approach [47, 55]. SU, where the bond update corresponds to a (computationally more tractable) global optimization problem, is exact in 1D and on the Husimi lattice, where the bonds have no additional environment [48, 57]. Figures 1(a), 2(a), and 2(b) of the main text compare the values of $E_0(D)$ and $M(D)$ obtained by the SU and FU techniques. The SU approach clearly overestimates the expectation value of a local observable, and can be regarded as providing an upper bound. How-

ever, the key information is that the computational cost of the FU approach prohibits its use beyond $D = 13$, whereas SU can be employed to at least double this value. Because the behavior of $E_0(D)$ and $M(D)$ obtained by SU is very similar to the more efficient FU, and the much greater D delivers far superior estimates of both [Figs. 1(a), 2(a), and 2(b)], we rely on SU for our primary conclusions.

Another fundamental, and valuable, degree of freedom within the PESS construction is the choice of the simplex to use, with larger simplices delivering more accurate results [55]. Here we gauge the effects of the simplex by comparing our 3-PESS results with those from a 9-PESS Ansatz [Figs. 1(a), 2(a), and 2(b)]. However, when each procedure is optimized, the larger simplices incur the penalty that the maximum accessible D is lower. A further variable in our calculations is the size of the unit cell for which translational invariance is assumed; ordered states and those with large local bound states may clearly be favored or penalized by different choices of unit cell. The unit cell can be any multiple of the simplex size, and we have run our 3-PESS calculations for 3-, 9-, and 12-site unit cells. Our 9-PESS calculations are made only with a 1-simplex (9-site) unit cell, but because this accommodates both the $q = 0$ and $\sqrt{3} \times \sqrt{3}$ ordering patterns, we believe that no bias is introduced. When the starting Hamiltonian is extended to the J_1 - J_2 model, this can in principle be computed in the 3-PESS formalism, but here the J_2 bond is an inter-simplex connection. This makes for a very much less efficient projection and update procedure, significantly reducing the range of available D values. Thus all of the J_1 - J_2 results we report were obtained in the 9-PESS framework.

Calculation of Expectation Values

The calculation of a physical expectation value from a PESS representation with bond dimension D requires in general the full summation over a two-dimensional reduced tensor network with bond dimension D^2 . This becomes the primary bottleneck at larger D in most tensor-network algorithms [49]. We have developed a new approach to this problem, which is based on the conventional time-evolving block decimation (TEBD) technique for performing the summation [50], but avoids calculating the reduced tensor network by obtaining the expectation values directly from the local tensors in the PESS representation [51]. By comparison with the TEBD method in two dimensions, the new method reduces both the computational and memory costs by two orders of D , i.e. from D^{10} to D^8 and from D^8 to D^6 respectively. Thus we are able to extend the calculation of some expectation values as far as $D = 30$ ($D = 25$ with full statistical reliability). This extended range is very important for the kagome Heisenberg antiferromagnet because of the ex-

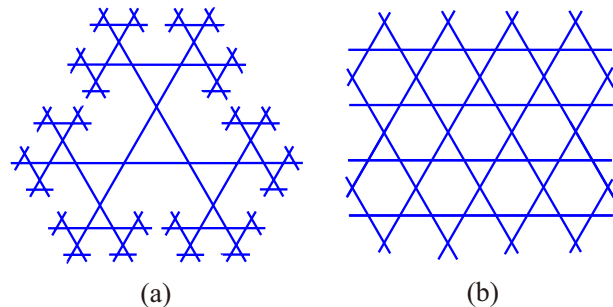


FIG. S1. (a) Triangular Husimi lattice. (b) Kagome lattice.

tremely slow convergence of $E_0(D)$ and $M(D)$ [Figs. 1(a), 1(b), 2(a), and 2(b)].

We gauge the reliability of our results by considering the truncation error in $E_0(D)$ and $M(D)$ as functions of D_{mps} . We comment that the TNS wave function obtained by repeated TEBD projection is fully variational, and as such increasing D leads to a lower energy estimate [Fig. 1(a)]. However, the evaluation of physical expectation values is not a variational procedure, because the MPS basis is changed for each value of D_{mps} and is not determined by minimizing the energy. Thus an increase of D_{mps} in the evaluation step [Fig. 1(c)] should be considered only as improving the accuracy of the expectation value being estimated.

III. On the relationship between Husimi and kagome magnetizations

While there exists to our knowledge no analytical proof that the magnetization of the Husimi lattice at finite bond dimension, $M_{\text{H}}(D)$, should be an upper bound on the magnetization of the kagome lattice, $M_{\text{k}}(D)$, for the same value of D , here we present a heuristic argument. The triangular Husimi lattice [Fig. S1(a)] is a kagome lattice [Fig. S1(b)] with no longer loops, i.e. all of the hexagons and longer paths, meaning those with $N > 6$ bonds, of the kagome lattice are simply absent due to the lack of connectivity of the Husimi lattice. These loops are mutually frustrating for joint spin-rotation processes. In a local picture, the short, even-length loops offer extensive possibilities for gains in resonance energy due to spin fluctuations, and in a gapless state long loops may also be involved. By contrast, no further energy is gained if the spins retain their 120-degree configuration, because the two lattices have equal numbers of bonds per site. Thus the only possible effect of loop processes on the finite- D magnetization should be to suppress it, with the result that $M_{\text{H}}(D) > M_{\text{k}}(D)$. Figures 2(a) and 2(b) of the main text present a clear numerical demonstration of this inequality.